

# Electronic transport properties of an (8, 0) carbon/silicon-carbide nanotube heterojunction\*

Liu Hongxia(刘红霞)<sup>1,†</sup>, Zhang Heming(张鹤鸣)<sup>1</sup>, and Zhang Zhiyong(张志勇)<sup>2</sup>

(1 Key Laboratory of the Ministry of Education for Wide Band-Gap Semiconductor Materials and Devices, School of Microelectronics, Xidian University, Xi'an 710071, China)

(2 Institute of Information Science and Technology, Northwest University, Xi'an 710069, China)

**Abstract:** A two-probe system of the heterojunction formed by an (8, 0) carbon nanotube (CNT) and an (8, 0) silicon carbide nanotube (SiCNT) was established based on its optimized structure. By using a method combining nonequilibrium Green's function (NEGF) with density functional theory (DFT), the transport properties of the heterojunction were investigated. Our study reveals that the highest occupied molecular orbital (HOMO) has a higher electron density on the CNT section and the lowest unoccupied molecular orbital (LUMO) mainly concentrates on the interface and the SiCNT section. The positive and negative threshold voltages are +1.8 and -2.2 V, respectively.

**Key words:** carbon/silicon carbide nanotube heterojunction; nonequilibrium Green's function; transport properties

**DOI:** 10.1088/1674-4926/30/5/052002

**PACC:** 7115M; 7125X; 6600

## 1. Introduction

One-dimensional heterojunctions, especially nanotube heterojunctions, have attracted tremendous interest owing to their distinctive structures and properties, which are of crucial importance for both scientific fundamentals in nanoscience and potential applications in nanoelectronics<sup>[1]</sup>. Most of the fabricated nanotube heterojunctions are formed between a bulk material and a nanotube<sup>[2-6]</sup>. Meanwhile, the heterojunctions formed by nanotubes are rarely studied. This is due to the difficulties in their fabrication. With the development of the synthesis technology in nano-materials, the heterojunction constructed from a carbon nanotube and the nitrogen-doped carbon nanotube have been successfully prepared<sup>[7]</sup>. CNT heterojunction arrays have been fabricated via successive plasma-enhanced chemical vapor deposition<sup>[8]</sup>.

The method combining nonequilibrium Green's function (NEGF) with density functional theory (DFT) has been widely used in molecular devices<sup>[9-12]</sup>. Furthermore, this method is also applied in CNT nanoelectronics. The influence of the size of the CNT heterojunction on the transport properties has been studied with this method<sup>[13]</sup>. Bai *et al.* investigated the carbon nanotube diode and achieved rectifying properties<sup>[14]</sup>. When several carbon nanotubes are used to form the channel of the CNT field effect transistors (CNTFETs), the coupling effect between adjacent nanotubes seriously influences the performances of the CNTFETs<sup>[15]</sup>.

In this work, the transport properties of the heterojunction formed by an (8, 0) CNT and an (8, 0) SiCNT are investigated with a method combining NEGF with DFT. Our results show that the highest occupied molecular orbital (HOMO) of the heterojunction has a higher electron density on the CNT section and the lowest unoccupied molecular orbital (LUMO) mainly concentrates on the interface and the SiCNT

section. The current-voltage curve of the heterojunction has two steep increases at +1.8 and -2.2 V. The maximal positive and negative currents are +48 and -32  $\mu\text{A}$ , respectively. Our investigations are helpful for the modeling of a nanotube heterojunction.

## 2. Model and method

The structure of the heterojunction is key to its transport properties. In this paper, the structure was achieved through geometry optimization based on first-principle calculations and performed with the CASTEP package<sup>[16]</sup>. For the geometry optimization, the heterojunction was placed in a supercell, as shown in Fig. 1, and the maximal force, stress, and displacement were set to be 0.05 eV/Å, 0.05 GPa, and  $5 \times 10^{-4}$  Å.

By comparing the differences in radii between the heterojunction and the isolated nanotubes, the displacements at the heterojunction can be determined. The maximal diameter change of the CNT section is 1.088 Å in layer 9. For C layers further away from the interface of the junction, the deviation of the diameter decreases sharply. The variation of the third C layer (layer 7) is only 0.010 Å (about 0.16%), which is negligible. While in the SiCNT section, the SiCNT

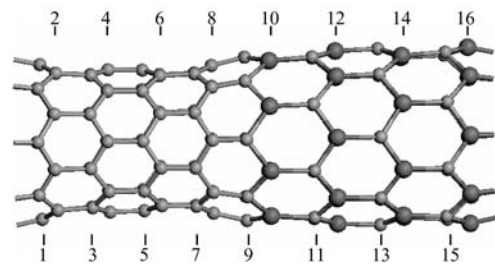


Fig. 1. Structure of the CNT/SiCNT heterojunction. The left part is the CNT section and the right part is the SiCNT section.

\* Project supported by the Pre-Research Foundation from the National Ministries and Commissions (No. 51308040203).

† Corresponding author. Email: liuhongxia\_xidian@126.com

Received 9 November 2008, revised manuscript received 28 December 2008

© 2009 Chinese Institute of Electronics

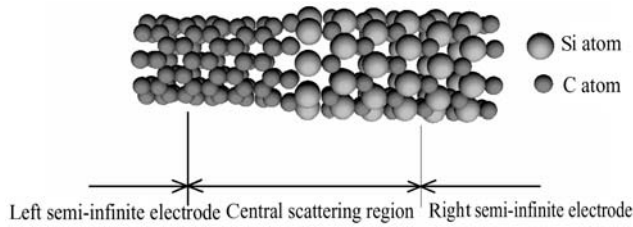


Fig. 2. Two-probe system for the CNT/SiCNT heterojunction.

diameter is slightly narrowed and the maximum change in the diameter occurs in layer 10 (about 3.268%). The changes in radius mainly occur at the interface and decrease sharply when moving away from the interface.

To study the transport properties of the heterojunction, a two-probe system of the heterojunction was constructed (Fig. 2), which can be divided into the left semi-infinite electrode, the central scattering region, and the right semi-infinite electrode. The structures of the left and right semi-infinite electrodes are the same as those of the individual CNT and SiCNT. The central scattering region consists of the heterojunction, shown in Fig. 1. The periodic boundary conditions were imposed on the plane perpendicular to the axis of the nanotubes. Through an analysis of the optimized structure of the heterojunction, it can be seen that our model is large enough for the study of its transport properties.

The transport properties of the above two-probe system were explored using the nonequilibrium Green's function method implemented in the Transiesta-C package and its latest version, Atomistix ToolKit 2.3 (ATK 2.3). This method has been successfully applied in studies of the transport properties of molecular devices. In our calculations, a local density approximation was adopted to describe the exchange-correlation energy. The valence electrons were expanded in a numerical atomic-orbital basis set of single zeta (SZ). The core electrons were modeled using Troullier–Martins local pseudopotentials<sup>[17]</sup>.

The transmission spectrum and the current–voltage characteristics are of great importance for the electronic transport properties of molecular devices. The transmission spectrum describes the probability for electron with incident energy  $E$  to transfer from the left semi-infinite electrode to the right electrode and is calculated by

$$T(E, V) = T_r[\Gamma_L(E, V)G(E, V)\Gamma_R(E, V)G^\dagger(E, V)], \quad (1)$$

where  $G(E, V)$  is Green's function of the two-probe system, and  $\Gamma_{L/R}$  is the coupling matrix. The integral of the transmission spectrum yields the current through the system:

$$I(V) = \int_{\mu_L}^{\mu_R} T(E, V)[f(E - \mu_L) - f(E - \mu_R)]dE, \quad (2)$$

where  $\mu_L = -V/2$  and  $\mu_R = V/2$  are the chemical potential of the left and right electrodes, respectively.

### 3. Results and discussion

The equilibrium transport properties (no bias voltage applied) of the two-probe system were studied first. The trans-

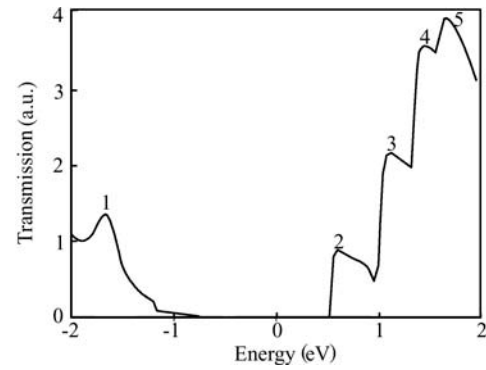


Fig. 3. Transmission spectrum of the two-probe system for the heterojunction.

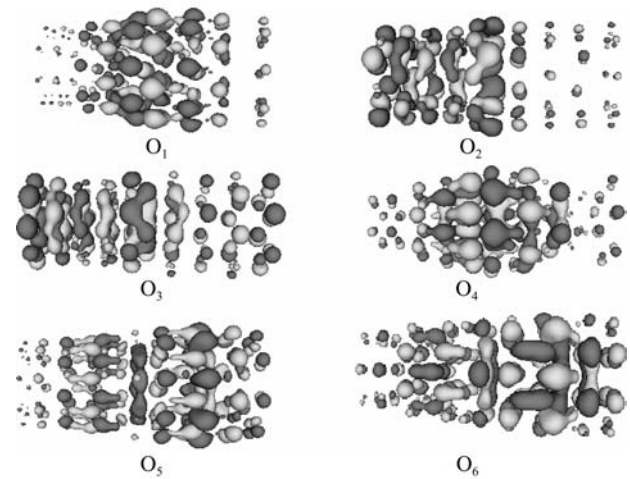


Fig. 4. Frontier orbitals of the MPSH for the heterojunction.

mission coefficient  $T(E)$  for the heterojunction as a function of energy is plotted in Fig. 3. There are five peaks marked in the transmission spectrum. A transmission gap of about 1.20 eV can be found, which means that in this energy range the possibility of an electron to transfer from one electrode to another is nearly zero.

The molecular projected self-consistent Hamiltonian (MPSH) can be achieved by projecting the self-consistent Hamiltonian onto the Hilbert space spanned by the basis functions of the central atoms. The eigenstates of the MPSH are associated with the poles of Green's function and roughly correspond to the peaks in the transmission spectrum<sup>[9]</sup>. To understand the peaks in Fig. 3, we calculated the frontier molecular orbitals of the MPSH for the heterojunction.

Figure 4 shows the six frontier molecular orbitals of the MPSH for the heterojunction. The orbital  $O_1$  is the LUMO, which has a higher density on the interface and the SiCNT section. The orbital  $O_2$  is the HOMO and has a higher electron density on the CNT section. As the locality of these two orbitals is high, no transmission peaks are formed by them. The orbitals  $O_3$  and  $O_4$  correspond to the transmission peaks 1 and 2 shown in Fig. 3, respectively. Since the locality of  $O_4$  is higher than that of  $O_3$ , the magnitude of the transmission peak 1 is higher than that of the transmission peak 2. Transmission peaks 3 and 4 are related to the orbitals  $O_5$  and  $O_6$ , which have eigenvalues of 1.19 and

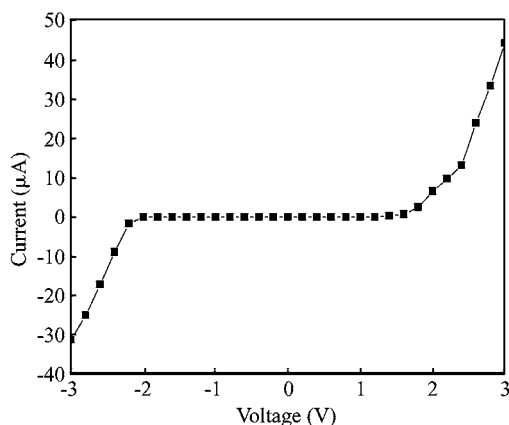


Fig. 5. Current–voltage curve of the two-probe system for CNT/SiCNT heterojunction.

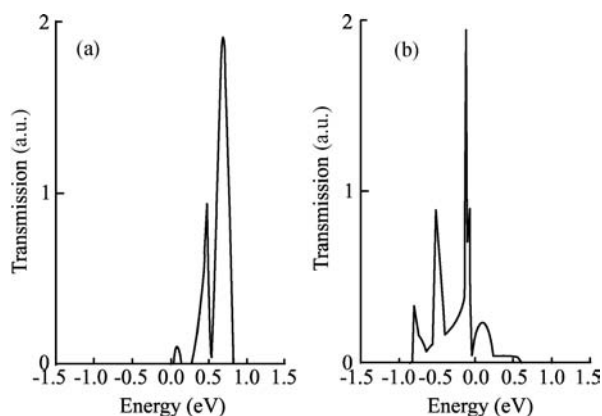


Fig. 6. Transmission spectra of the heterojunction under a bias of (a)  $V = -2.6$  V and (b)  $V = +2.6$  V.

1.58 eV, respectively.

The current as a function of the applied bias voltage for the heterojunction is presented in Fig. 5. For each bias voltage, the electronic structure is determined self-consistently under nonequilibrium conditions. The current is calculated by the Landauer–Büttiker formula: [Eq. (2)], which is determined by the transmission probability  $T(E,V)$  and the energy region (or integral window) of the current integral. Setting the Fermi level to zero, the integral window is  $[-V/2, V/2]$ . As the calculation of the current is very time consuming, the bias range is limited from  $-3.0$  to  $3.0$  V.

The  $I$ – $V$  curve of the heterojunction (Fig. 5) can be divided into three regions. In the bias region from  $-2.2$  to  $+1.8$  V, the current is nearly zero, which means the transmission probability  $T(E,V)$  in the integral window is zero. While the bias voltage is greater than  $-2.2$  or  $+1.8$  V, the current increases with an increase in voltage. To understand the reason for the increase of the current, the transmission spectra of the heterojunction under biases of  $-2.6$  and  $+2.6$  V were calculated and plotted in Fig. 6.

In the transmission spectrum of the heterojunction under a bias  $V = -2.6$  V (Fig. 6(a)), there are two transmission peaks at energies of 0.48 and 0.68 eV. The current is influenced by these two peaks. The corresponding frontier molecular orbitals of the MPSH were calculated and labeled as  $O_7$  and  $O_8$

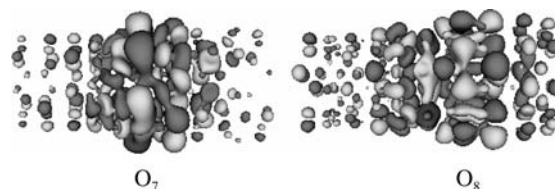


Fig. 7. Frontier orbitals of the MPSH under a bias of  $V = -2.6$  V.

in Fig. 7. The localization of the two orbitals is low, meaning that the transport probability of electrons is high and the current contributed by these orbitals is large. The reason for the increase of the current under the positive bias voltage follows the same argumentation.

## 4. Conclusions

To investigate the transport properties of the heterojunction formed by CNT and SiCNT, the structure of the heterojunction was first obtained through a geometry optimization. Based on the optimized structure, a two-probe system of the heterojunction was designed. Its transport properties were calculated with a method combining NEGF with DFT. The results show that the HOMO and the LUMO of the heterojunction have higher electron densities in the CNT section and the SiCNT section, respectively. The increase of the current at voltages larger than  $+1.8$  and  $-2.2$  V results from the formation of new transmission peaks, or in other words by the opening of new conducting channels. Our calculations are helpful for the modeling of nanotube heterojunction electronic devices.

## Acknowledgements

We wish to thank Atomistix for the use of the trial version of Atomistix ToolKit 2.3 (ATK 2.3).

## References

- [1] Qi Xiang, Bao Qiaoliang, Li Changming, et al. Spark plasma sintering-fabricated one-dimensional nanoscale “crystalline-amorphous” carbon heterojunction. *Appl Phys Lett*, 2008, 92: 113113
- [2] Hu Jiangtao, Ouyang Min, Yang Peidong, et al. Controlled growth and electrical properties of heterojunctions of carbon nanotubes and silicon nanowires. *Nature*, 1999, 399: 48
- [3] Zhang Y, Ichihashi T, Landree E, et al. Heterostructures of single-walled carbon nanotubes and carbide nanorods. *Science*, 1999, 285(5434): 1719
- [4] Wu Yiyang, Fan Rong, Yang Peidong. Block-by-block growth of single-crystalline Si/SiGe superlattice nanowires. *Nano Lett*, 2002, 2(2): 83
- [5] Björk M T, Ohlsson B J, Sass T, et al. One-dimensional steeplechase for electrons realized. *Nano Lett*, 2002, 2(2): 87
- [6] Gudiksen M S, Lauhon L J, Wang J, et al. Growth of nanowire superlattice structures for nanoscale photonics and electronics. *Nature*, 2002, 415: 617
- [7] Chai Y, Zhou X L, Li P J, et al. Nanodiode based on a multi-wall  $CN_x$ /carbon nanotube intramolecular junction. *Nanotechnology*, 2005, 16(10): 2134

- [8] Cassell A M, Li J, Stevens R M D, et al. Vertically aligned carbon nanotube heterojunctions. *Appl Phys Lett*, 2004, 85(12): 2364
- [9] Li Z, Kosov D S. Dithiocarbamate anchoring in molecular wire junction: a first principles study. *J Phys Chem B*, 2006, 110(20): 9893
- [10] Sen S, Chakrabarti S. Ab initio density functional study on negative differential resistance in a fused furan trimer. *J Phys Chem C*, 2008, 112(5): 1685
- [11] Cohen R, Stokbro K, Martin J M L, et al. Charge transport in conjugated aromatic molecular junctions: molecular conjugation and molecule-electrode coupling. *J Phys Chem C*, 2007, 111(40): 14893
- [12] Long Mengqiu, Chen Keqiu, Wang Lingling, et al. Negative differential resistance induced by intermolecular interaction in a bimolecular device. *Appl Phys Lett*, 2007, 91(23): 233512
- [13] Li Xiaofei, Chen Keqiu, Wang Lingling, et al. Effect of length and size of heterojunction on the transport properties of carbon-nanotube devices. *Appl Phys Lett*, 2007, 91(13): 133511
- [14] Bai P, Li E, Lam K T, et al. Carbon nanotube Schottky diode: an atomic perspective. *Nanotechnology*, 2008, 19(11): 115203
- [15] Li Xiaofei, Chen Keqiu, Wang Lingling, et al. Effect of inter-tube interaction on the transport properties of a carbon double-nanotube device. *J Appl Phys*, 2007, 101(6): 064514
- [16] Watanabe K, Sakairi M, Takahashi H, et al. Anodizing of aluminum coated with silicon oxide by a sol-gel method. *J Electrochem Soc*, 2001, 148(11): B473
- [17] Troullier N, Martins J L. Efficient pseudopotentials for plane-wave calculations. *Phys Rev B*, 1991, 43(3): 1993